Discontinuous Galerkin Subgrid Finite Element Method for Heterogeneous Brinkman's Equations

Oleg P. Iliev[1,2], Raytcho D. Lazarov[2,3], and Joerg Willems[1,3]

[1]Fraunhofer ITWM, Kaiserslautern, Germany
[2]Inst. Mathematics, Bulgarian Academy of Sciences, Sofia, Bulgaria
[3]Dept. Mathematics, Texas A&M University, College Station, TX 77843, USA

Abstract. We present a two-scale finite element method for solving Brinkman's equations with piece-wise constant coefficients. This system of equations model fluid flows in highly porous, heterogeneous media with complex topology of the heterogeneities. We make use of the recently proposed discontinuous Galerkin FEM for Stokes equations by Wang and Ye in [12] and the concept of subgrid approximation developed for Darcy's equations by Arbogast in [4]. In order to reduce the error along the coarse-grid interfaces we have added a alternating Schwarz iteration using patches around the coarse-grid boundaries. We have implemented the subgrid method using Deal.II FEM library, [7], and we present the computational results for a number of model problems.

Key words: numerical upscaling, flow in heterogeneous porous media, Brinkman equation, subgrid approximation, mixed FEM

1 Introduction

In this paper we consider the Brinkman's equations for the velocity $\boldsymbol{u}$ and the pressure p:

$$\begin{aligned} -\mu\Delta\boldsymbol{u} + \nabla p + \mu\kappa^{-1}\boldsymbol{u} &= \boldsymbol{f} \quad \text{in } \Omega, \\ \nabla\cdot\boldsymbol{u} &= 0 \quad \text{in } \Omega, \\ \boldsymbol{u} &= \boldsymbol{0} \quad \text{on } \partial\Omega. \end{aligned} \tag{1}$$

Here $\mu > 0$ is the viscosity, Ω is a bounded simply connected domain in $\mathbb{R}^n$, $n = 2, 3$, with Lipschitz polyhedral boundary having the outward unit normal vector $\boldsymbol{n}$, $0 < \kappa \in L^\infty(\Omega)$ is the permeability and $\boldsymbol{f} \in L^2(\Omega)^n$ is a forcing term. Then problem (1) has unique weak solution $(\boldsymbol{u}, p) \in (H^1(\Omega)^n, L_0^2(\Omega))$.

Brinkman's equations adequately describe flows in highly porous media. They are used for modeling many industrial materials and processes such as industrial filters, with porosity above 0.9, thermal insulators made of glass or mineral wool with porosity 0.99, or open foams with porosity above 0.95, see Fig. 1. Equation (1) was introduced by Brinkman in [6] in order to reduce the deviations between the measurements for flows in highly porous media and the Darcy-based predictions. This was done without direct link to underlying microscopic behavior

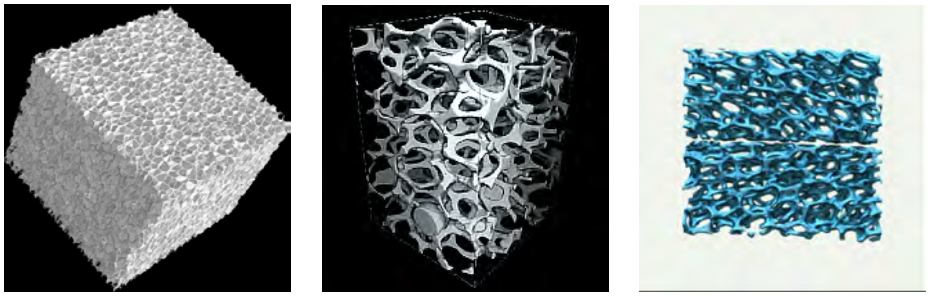

Fig. 1. Microstructure of industrial foams

of the flow process, but as a constitutive relation involving a dissipative term scaled by the viscosity. However, advances in homogenization theory made it possible to rigorously derive Brinkman's equations from Stokes' equations in the case of slow viscous fluid flow in the presence of periodically arranged solid obstacles, see e.g., [1, 2, 9, 11]. Also, system (1) has been considered from the point of view of fictitious domain or penalty formulation of flows of incompressible liquids around solid or porous obstacles; in this case the coefficients are piece-wise constant: the viscosity μ is constant and κ is "small" in the solid obstacles and "infinity" in the fluid, (see, e.g. [3]).

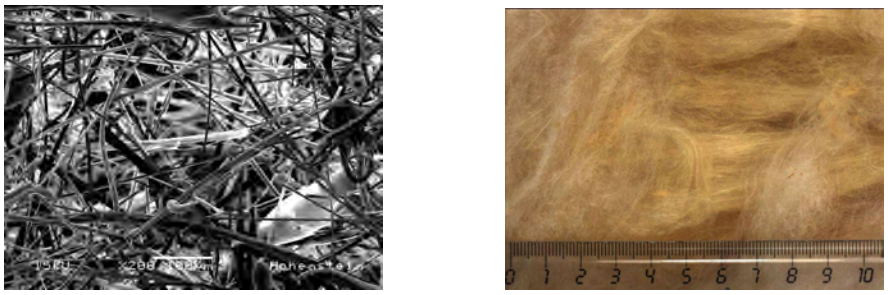

Fig. 2. Microstructure and marcostructure of mineral wool

In this paper we derive and study numerical methods for solving Brinkman's equations (1) assuming that the coefficient κ is piece-wise constant and has large jumps. Moreover, the structure of the subdomains, where the coefficient is constant, has quite a complicated geometry, see, e.g. Figure 1. For such problems we shall construct and numerically test two-scale finite element approximations. In the case of problems with scale separation the method captures well the coarse scale behavior of the solution and enhances it with fine scale features. Also, we extend such approximations to numerically treat problems without scale separation. Enhancing the method by subdomains around the coarse-grid

edges we devise an iterative alternating Schwarz methods, which converges to the fine-grid approximate solution. All constructions are implemented within the Deal.II finite element library. As a byproduct of this development we also obtaine a subgrid finite element approximation of Darcy's problem, a method proposed and justified by Arbogast [4], and the discontinuous Galerkin method for Stokes' equations, proposed and studied by Wang and Ye [12].

In this note we present derivation of a subgrid approximation of Brinkman equations and test the method on a number of model problems. Our further goals include theoretical and practical study of the error of the method, testing its performance on more realistic three-dimensional problems, and development and justification of efficient solution methods.

2 Preliminaries

Here we use the standard notation for spaces of scalar and vector-functions defined on Ω. $L^2(\Omega)$ is the space of measurable square integrable functions in Ω and $L^2_0(\Omega)$ is its subspace of functions with mean value zero. The Sobolev spaces $H^1(\Omega)$ and $H^1(\Omega)^n$ consist of scalar and vector-functions, respectively, with weak first derivatives in $L^2(\Omega)$ and $L^2(\Omega)^n$. Similarly,

$$H^1_0(\Omega)^n := \{\boldsymbol{v} \in H^1(\Omega)^n : \ \boldsymbol{v} = 0 \text{ on } \partial\Omega\},$$

$$H(div;\Omega) := \{\boldsymbol{v} \in L^2(\Omega)^n \ : \nabla \cdot \boldsymbol{v} \in L^2(\Omega)\},$$

$$H_0(div;\Omega) := \{\boldsymbol{v} \in H(div;\Omega) : \ \boldsymbol{v} \cdot \boldsymbol{n} = 0 \text{ on } \partial\Omega\}.$$

Further, P_k denotes the set of polynomials of degree $k \geq 0$ and P_k^n the set of vector functions in $\mathbb{R}^n$ with components in P_k.

The two-scale finite element method uses various (mixed) finite element spaces, which are defined below. Let $\mathcal{T}_H$ and $\mathcal{T}_h$ be quasi-uniform quadrilateral triangulations of Ω with mesh-parameter H and h, respectively, such that each $T_H \in \mathcal{T}_H$ is an agglomeration of elements in $\mathcal{T}_h$. We will refer to $\mathcal{T}_H$ and $\mathcal{T}_h$ as coarse and fine triangulation, respectively. Let $\mathcal{E}_H$ denote the set of all edges ($n = 2$) and faces ($n = 3$) of $\mathcal{T}_H$, respectively. Also, we define $\mathring{\mathcal{E}}_H$ to be the set of all internal edges/faces of $\mathcal{T}_H$, i.e., $\mathring{\mathcal{E}}_H := \{e_H \in \mathcal{E}_H |\ e_H \nsubseteq \partial\Omega\}$ and $\mathring{\mathcal{E}}_h$ to be the set of all edges/faces of $\mathcal{T}_h$ that are internal for the coarse-grid cells $T_H \in \mathcal{E}_H$. Furthermore, for each $T_H \in \mathcal{T}_H$ we denote by $\mathcal{T}_h(T_H)$ the restriction of $\mathcal{T}_h$ to the coarse finite element T_H, $\mathcal{T}_h(T_H)$ is referred to as a fine triangulation of T_H.

We denote by $(\mathscr{V}_H, \mathscr{W}_H)$ and $(\mathscr{V}_h, \mathscr{W}_h)$ the mixed finite element spaces corresponding to $\mathcal{T}_H(\Omega)$ and $\mathcal{T}_h(\Omega)$, resprectively. Likewise, for each $T_H \in \mathcal{T}_H(\Omega)$ and $e_H \in \mathring{\mathcal{E}}_H$ let

$$(\delta\mathscr{V}_h(T_H), \delta\mathscr{W}_h(T_H)) \subset (H_0(div;T_H), L^2_0(T_H)) \tag{2}$$

be mixed finite element spaces corresponding to $\mathcal{T}_h(T_H)$. We also consider the direct sums of these local finite element spaces and set

$$(\delta\mathscr{V}_h, \delta\mathscr{W}_h) := \bigoplus_{T_H \in \mathcal{T}_H} (\delta\mathscr{V}_h(T_H), \delta\mathscr{W}_h(T_H)),$$

where functions in $(\delta\mathscr{V}_h(T_H), \delta\mathscr{W}_h(T_H))$ are extended by zero to $\Omega\backslash T_H$.We, furthermore, assume that the finite element spaces satisfy the following properties:

$$\nabla \cdot \delta\mathscr{V}_h = \delta\mathscr{W}_h \quad \text{and} \quad \nabla \cdot \mathscr{V}_H = \mathscr{W}_H, \tag{3a}$$

$$\delta\mathscr{W}_h \perp \mathscr{W}_H \quad \text{in the } L^2\text{-inner-product}, \tag{3b}$$

and

$$\mathscr{V}_H \cap \delta\mathscr{V}_h = \{\mathbf{0}\}. \tag{3c}$$

We note that if we choose $(\mathscr{V}_H, \mathscr{W}_H)$ and $(\delta\mathscr{V}_h(T_H), \delta\mathscr{W}_h(T_H))$, with $T_H \in \mathcal{T}_H$, to be Brezzi-Douglas-Marini (BDM1) mixed finite element spaces of order one (cf. e.g. [5, Section III.3, p. 126]), then (3) is satisfied. The velocity for the BDM1 space in 2-D is given by

$$P_1^2 + span\{curl(x_1^2 x_2),\ curl(x_1 x_2^2\} = P_1^2 + span\{(x_1^2, -2x_1x_2),\ (2x_1x_2, -x_2^2)\}$$

on each cell, with the restriction that the normal component is continuous across cell boundaries. In 3-D the spaces are defined in a similar manner, see, e.g. [5, Section III.3, p. 127]. Due to (3b) and (3c) the following direct sum is well-defined

$$(\mathscr{V}_{H,h}, \mathscr{W}_{H,h}) := (\mathscr{V}_H, \mathscr{W}_H) \oplus (\delta\mathscr{V}_h, \delta\mathscr{W}_h)\,. \tag{4}$$

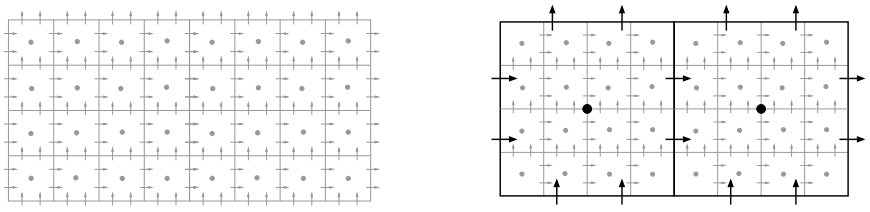

(a) $(\mathscr{V}_h, \mathscr{W}_h)$. (b) $(\mathscr{V}_{H,h}, \mathscr{W}_{H,h})$ with 2 coarse cells.

Fig. 3. Degrees of freedom of different mixed finite element spaces corresponding to BDM1 elements for the velocity and piece-wise constant functions for the pressure.

3 Subgrid Method for Brinkman's Equations

Now we outline the numerical subgrid approach for problem (1) in the way T. Arbogast applied it to Darcy's problem in [4].

It is well known that the mixed variational formulation of (1) reads as follows: Find $(\boldsymbol{u}, p) \in (H_0^1(\Omega)^n, L_0^2(\Omega))$ such that for all $(\boldsymbol{v}, q) \in (H_0^1(\Omega)^n, L_0^2(\Omega))$

$$a\,(\boldsymbol{u}, \boldsymbol{v}) + b\,(\boldsymbol{v}, p) + b\,(\boldsymbol{u}, q) = \int_\Omega \boldsymbol{f} \cdot \boldsymbol{v} d\boldsymbol{x}, \tag{5}$$

where

$$b\left(\boldsymbol{v},q\right):=-\int_{\Omega}\nabla\cdot\boldsymbol{v}qd\boldsymbol{x}, \tag{6a}$$

$$a\left(\boldsymbol{u},\boldsymbol{v}\right):=\int_{\Omega}(\mu\nabla\boldsymbol{u}:\nabla\boldsymbol{v}+\mu\kappa^{-1}\boldsymbol{u}\cdot\boldsymbol{v})d\boldsymbol{x}. \tag{6b}$$

Now we consider a finite element approximation of (5) with respect to $(\mathscr{V}_{H,h},\mathscr{W}_{H,h})$. Note, that $\mathscr{V}_{H,h}\not\subset H_0^1(\Omega)^n$, and therefore it is a nonconforming finite element space. However, we have that $\mathscr{V}_{H,h}\subset H_0(div;\Omega)$ and we can use the discontinuous Galerkin approximation of Stokes equations, derived in [12]: Find $(\boldsymbol{u}_{H,h},p_{H,h})\in(\mathscr{V}_{H,h},\mathscr{W}_{H,h})$ such that for all $(\boldsymbol{v}_{H,h},q_{H,h})\in(\mathscr{V}_{H,h},\mathscr{W}_{H,h})$ we have

$$a_h\left(\boldsymbol{u}_{H,h},\boldsymbol{v}_{H,h}\right)+b\left(\boldsymbol{v}_{H,h},p_{H,h}\right)+b\left(\boldsymbol{u}_{H,h},q_{H,h}\right)=F(\boldsymbol{v}_{H,h}), \tag{7}$$

where

$$\begin{aligned}a_h\left(\boldsymbol{u},\boldsymbol{v}\right):=&\sum_{T_h\in\mathcal{T}_h}\int_{T_h}\left(\nabla\boldsymbol{u}:\nabla\boldsymbol{v}+\kappa^{-1}\boldsymbol{u}\cdot\boldsymbol{v}\right)d\boldsymbol{x}\\&+\sum_{e\in\mathcal{E}_h}\int_e\left(\frac{\alpha}{|e|}\left[\!\left[\boldsymbol{u}\right]\!\right]\left[\!\left[\boldsymbol{v}\right]\!\right]-\left\{\!\left\{\varepsilon(\boldsymbol{u})\right\}\!\right\}\left[\!\left[\boldsymbol{v}\right]\!\right]-\left\{\!\left\{\varepsilon(\boldsymbol{v})\right\}\!\right\}\left[\!\left[\boldsymbol{u}\right]\!\right]\right)ds\end{aligned} \tag{8}$$

with the average $\left\{\!\left\{\varepsilon(\cdot)\right\}\!\right\}$ and the jump $\left[\!\left[\cdot\right]\!\right]$ defined by

$$\left\{\!\left\{\varepsilon(\boldsymbol{u})\right\}\!\right\}:=\begin{cases}\frac{1}{2}\left(\boldsymbol{n}^+\cdot\nabla(\boldsymbol{u}|_{T_h^+}\cdot\boldsymbol{\tau}^+)+\boldsymbol{n}^-\cdot\nabla(\boldsymbol{u}|_{T_h^-}\cdot\boldsymbol{\tau}^-)\right) & \text{on } e\in\mathring{\mathcal{E}}_h,\\ \boldsymbol{n}^+\cdot\nabla(\boldsymbol{u}|_{T_h^+}\cdot\boldsymbol{\tau}^+) & \text{on } e\in\mathcal{E}_h^{\partial}\end{cases} \tag{9a}$$

and

$$\left[\!\left[\boldsymbol{v}\right]\!\right]:=\begin{cases}\boldsymbol{v}|_{T_h^+}\cdot\boldsymbol{\tau}^+ + \boldsymbol{v}|_{T_h^-}\cdot\boldsymbol{\tau}^- & \text{on } e\in\mathring{\mathcal{E}}_h,\\ \boldsymbol{v}|_{T_h^+}\cdot\boldsymbol{\tau}^+ & \text{on } e\in\mathcal{E}_h^{\partial}.\end{cases} \tag{9b}$$

Here $\alpha>0$ is a sufficiently large stabilization parameter, $\boldsymbol{n}$ and $\boldsymbol{\tau}$ are normal and tangential vectors to the edge e (with right orientation), the superscripts $^+$ and $^-$ refer to the elements on either side of edge e, and $\mathring{\mathcal{E}}_h$ and $\mathcal{E}_h^{\partial}$ denote the sets of all internal and boundary edges, respectively.

If $H=h$, i.e. $\delta\mathscr{V}_h=\emptyset$, $\delta\mathscr{W}_h=\emptyset$, we have a single grid approximation of Brinkman's equations, a method proposed and studied by Wang and Ye in [12] for Stokes equations. The approximate solution obtained on a single grid for H sufficiently small will be further called a reference solution.

The subsequent derivation, which follows the reasoning in [4], is the core of the numerical subgrid approach and essentially yields a splitting of (7) into one coarse global and several fine local problems. Due to (4) we know that each element in $(\mathscr{V}_{H,h},\mathscr{W}_{H,h})$ may be uniquely decomposed into its components from $(\mathscr{V}_H,\mathscr{W}_H)$ and $(\delta\mathscr{V}_h,\delta\mathscr{W}_h)$. Thus, (7) may be rewritten as

$$\begin{aligned}a_h\left(\boldsymbol{u}_H+\delta\boldsymbol{u}_h,\boldsymbol{v}+\delta\boldsymbol{v}_h\right)+b\left(\boldsymbol{v}+\delta\boldsymbol{v}_h,p_H+\delta p_h\right)&=F(\boldsymbol{v}+\delta\boldsymbol{v}_h),\\ b\left(\boldsymbol{u}_H+\delta\boldsymbol{u}_h,q+\delta q_h\right)&=0,\\ \forall(\boldsymbol{v},q)\in(\mathscr{V}_H,\mathscr{W}_H)\text{ and }\forall(\delta\boldsymbol{v}_h,\delta q_h)&\in(\delta\mathscr{V}_h,\delta\mathscr{W}_h).\end{aligned} \tag{10}$$

By linearity we may decompose (10) into

$$a_h\left(\boldsymbol{u}_H+\delta\boldsymbol{u}_h,\boldsymbol{v}\right)+b\left(\boldsymbol{v},p_H+\delta p_h\right)+b\left(\boldsymbol{u}_H+\delta\boldsymbol{u}_h,q\right)=F(\boldsymbol{v}),\quad \forall(\boldsymbol{v},q)\in(\mathscr{V}_H,\mathscr{W}_H), \tag{11a}$$

$$a_h\left(\boldsymbol{u}_H+\delta\boldsymbol{u}_h,\delta\boldsymbol{v}_h\right)+b\left(\delta\boldsymbol{v}_h,p_H+\delta p_h\right)+b\left(\boldsymbol{u}_H+\delta\boldsymbol{u}_h,\delta q_h\right)=F(\delta\boldsymbol{v}_h),\quad \forall(\delta\boldsymbol{v}_h,\delta q_h)\in(\delta\mathscr{V}_h,\delta\mathscr{W}_h). \tag{11b}$$

Due to (3a), (3b), and (3c) we may simplify (11) to obtain the equation:

$$a_h\left(\boldsymbol{u}_H+\delta\boldsymbol{u}_h,\boldsymbol{v}\right)+b\left(\boldsymbol{v},p_H\right)+b\left(\boldsymbol{u}_H,q\right)=F(\boldsymbol{v})\quad \forall\ (\boldsymbol{v},q)\in(\mathscr{V}_H,\mathscr{W}_H) \tag{12a}$$

$$a_h\left(\boldsymbol{u}_H+\delta\boldsymbol{u}_h,\delta\boldsymbol{v}_h\right)+b\left(\delta\boldsymbol{v}_h,\delta p_h\right)+b\left(\delta\boldsymbol{u}_h,\delta q_h\right)=F(\delta\boldsymbol{v}_h),\quad \forall\ (\delta\boldsymbol{v}_h,\delta q_h)\in(\delta\mathscr{V}_h,\delta\mathscr{W}_h). \tag{12b}$$

Remark 1. This last step is crucial to ensure the solvability of (12b). In fact, the equivalence of (11b) and (12b) is a major reason for requiring the properties of the finite element spaces in (3). The requirements (3), however, significantly limit the possible choices of finite elements that might be used in the subgrid method.

Now, by further decomposing $(\delta\boldsymbol{u}_h,\delta p_h)=(\overline{\delta\boldsymbol{u}}_h+\widetilde{\delta\boldsymbol{u}}_h,\overline{\delta p}_h+\widetilde{\delta p}_h)$ and using superposition, (12b) may be replaced by the following systems of equations satisfied by $(\widetilde{\delta\boldsymbol{u}}_h,\widetilde{\delta p}_h)$ and $(\overline{\delta\boldsymbol{u}}_h,\overline{\delta p}_h)$, respectively, for all $(\delta\boldsymbol{v}_h,\delta q_h)\in(\delta\mathscr{V}_h,\delta\mathscr{W}_h)$:

$$a_h\left(\boldsymbol{u}_H+\widetilde{\delta\boldsymbol{u}}_h,\delta\boldsymbol{v}_h\right)+b\left(\delta\boldsymbol{v}_h,\widetilde{\delta p}_h\right)+b\left(\widetilde{\delta\boldsymbol{u}}_h,\delta q_h\right)=0 \tag{13a}$$

and

$$a_h\left(\overline{\delta\boldsymbol{u}}_h,\delta\boldsymbol{v}_h\right)+b\left(\delta\boldsymbol{v}_h,\overline{\delta p}_h\right)+b\left(\overline{\delta\boldsymbol{u}}_h,\delta q_h\right)=F(\delta\boldsymbol{v}_h). \tag{13b}$$

We easily see by (13a) that $(\widetilde{\delta\boldsymbol{u}}_h,\widetilde{\delta p}_h)=(\widetilde{\delta\boldsymbol{u}}_h(\boldsymbol{u}_H),\widetilde{\delta p}_h(\boldsymbol{u}_H))$ is a linear operator in $\boldsymbol{u}_H$. Unfortunately, as written, these two problems do not lead to local (over the coarse elements) computations since they are connected through the penalty involving the tangential component of $\widetilde{\delta\boldsymbol{u}}_h$ and $\overline{\delta\boldsymbol{u}}_h$ on ∂T_H. We achieve the desired localization by considering equations (13) over each coarse grid cell with zero tangential component of the velocity imposed weakly by the penalty term (for more details, see [13]). Keeping this in mind we further use the same notation. In the following we refer to $(\overline{\delta\boldsymbol{u}}_h,\overline{\delta p}_h)$ and $(\widetilde{\delta\boldsymbol{u}}_h(\boldsymbol{u}_H),\widetilde{\delta p}_h(\boldsymbol{u}_H))$ as the responses to the right hand side and $\boldsymbol{u}_H$, respectively.

Plugging $\overline{\delta\boldsymbol{u}}_h+\widetilde{\delta\boldsymbol{u}}_h(\boldsymbol{u}_H)$ into (12a) we arrive at an upscaled equation, which is entirely posed in terms of the coarse unknowns, i.e. for all $(\boldsymbol{v},q)\in(\mathscr{V}_H,\mathscr{W}_H)$

$$\begin{aligned} a_h\left(\boldsymbol{u}_H+\widetilde{\delta\boldsymbol{u}}_h(\boldsymbol{u}_H),\boldsymbol{v}\right)+b\left(\boldsymbol{v},p_H\right)&=F(\boldsymbol{v})-a_h\left(\overline{\delta\boldsymbol{u}}_h,\boldsymbol{v}\right),\\ b\left(\boldsymbol{u}_H,q\right)&=0.\end{aligned} \tag{14}$$

Now, due to the first equation in (13a) we see, by choosing $\delta\boldsymbol{v}_h=\widetilde{\delta\boldsymbol{u}}_h(\boldsymbol{v})$, that

$$a_h\left(\boldsymbol{u}_H+\widetilde{\delta\boldsymbol{u}}_h(\boldsymbol{u}_H),\widetilde{\delta\boldsymbol{u}}_h(\boldsymbol{v})\right)+b\left(\widetilde{\delta\boldsymbol{u}}_h(\boldsymbol{v}),\widetilde{\delta p}_h(\boldsymbol{u}_H)\right)=0.$$

The second equation in (13a) in turn yields $b\left(\widetilde{\delta \boldsymbol{u}}_h(\boldsymbol{v}), \widetilde{\delta p}_h(\boldsymbol{u}_H)\right) = 0$ for any $\boldsymbol{v} \in \mathscr{V}_H$. Combining these two results with (14) we obtain the symmetric upscaled problem: find $(\boldsymbol{u}_H, p_H) \in (\mathscr{V}_H, \mathscr{W}_H)$ so that for all $(\boldsymbol{v}, q) \in (\mathscr{V}_H, \mathscr{W}_H)$

$$a_h\left(\boldsymbol{u}_H + \widetilde{\delta \boldsymbol{u}}_h(\boldsymbol{u}_H), \boldsymbol{v} + \widetilde{\delta \boldsymbol{u}}_h(\boldsymbol{v})\right) + b\left(\boldsymbol{v}, p_H\right) + b\left(\boldsymbol{u}_H, q\right) = F(\boldsymbol{v}) - a_h\left(\overline{\delta \boldsymbol{u}}_h, \boldsymbol{v}\right), \tag{15}$$

One can set up this linear system by first computing the responces $\widetilde{\delta \boldsymbol{u}}_h(\boldsymbol{u}_H)$ with $\boldsymbol{u}_H$ being a coarse-grid basis function. This could be done in advance and in parallel. Once (15) is solved for $(\boldsymbol{u}_H, p_H)$ we obtain the solution of (7) by

$$(\boldsymbol{u}_{H,h}, p_{H,h}) = (\boldsymbol{u}_H + \widetilde{\delta \boldsymbol{u}}_h(\boldsymbol{u}_H) + \overline{\delta \boldsymbol{u}}_h, p_H + \widetilde{\delta p}_h(\boldsymbol{u}_H) + \overline{\delta p}_h). \tag{16}$$

4 Subgrid Method and Alternating Schwarz Iterations

As noted in the previous section we presented a special way of computing the solution of (7), i.e., the finite element solution corresponding to the space $(\mathscr{V}_{H,h}, \mathscr{W}_{H,h})$. The difference between the spaces $(\mathscr{V}_{H,h}, \mathscr{W}_{H,h})$ and $(\mathscr{V}_h, \mathscr{W}_h)$ is that the former has no fine degrees of freedom across coarse cell boundaries. Thus, fine-scale features of the solution $(\boldsymbol{u}, p)$ across those coarse cell boundaries are poorly captured by functions in $(\mathscr{V}_{H,h}, \mathscr{W}_{H,h})$. Algorithm 1 addresses this problem by performing alternating Schwarz iterations between the spaces $(\mathscr{V}_{H,h}, \mathscr{W}_{H,h})$ and $(\mathscr{V}_h^\tau(e_H), \mathscr{W}_h^\tau(e_H))$ that consist of fine-grid functions defined on overlapping subdomains around each coarse-mesh interface $e_H \in \mathring{\mathcal{E}}_H$ of size H. Now, problem (17) is of exactly the same form as (7). Thus, by the same

Algorithm 1 Alternating Schwarz extension to the numerical subgrid approach for Darcy's problem – first formulation.

1: Set $(\boldsymbol{u}_h^0, p_h^0) \equiv (\boldsymbol{0}, 0)$.
2: **for** $j = 0, \ldots$ until convergence **do**
3: **if** $j > 0$ **then**
4: Starting from $(\boldsymbol{u}_h^j, p_h^i)$ perform an additive Schwarz step with respect to $(\mathscr{V}_h^\tau(e_H), \mathscr{W}_h^\tau(e_H))$ for all $e_H \in \mathcal{E}_H$ to get $(\boldsymbol{u}_h^{j+1/3}, p_h^{j+1/3})$.
5: **else**
6: $(\boldsymbol{u}_h^{1/3}, p_h^{1/3}) = (\boldsymbol{u}_h^0, p_h^0)$
7: **end if**
8: Find $(\boldsymbol{e}_{H,h}, e_{H,h}) \in (\mathscr{V}_{H,h}, \mathscr{W}_{H,h})$ such that for all $(\boldsymbol{v}, q) \in (\mathscr{V}_{H,h}, \mathscr{W}_{H,h})$ we have

$$\begin{cases} a_h\left(\boldsymbol{e}_{H,h}, \boldsymbol{v}\right) + b\left(\boldsymbol{v}, e_{H,h}\right) = F(\boldsymbol{v}) - a_h\left(\boldsymbol{u}_h^{j+1/3}, \boldsymbol{v}\right) - b\left(\boldsymbol{v}, p_h^{j+1/3}\right), \\ b\left(\boldsymbol{e}_{H,h}, q\right) = -b\left(\boldsymbol{u}_h^{j+1/3}, q\right). \end{cases} \tag{17}$$

9: Set

$$(\boldsymbol{u}_h^{j+1}, p_h^{j+1}) = (\boldsymbol{u}_h^{j+1/3}, p_h^{j+1/3}) + (\boldsymbol{e}_{H,h}, e_{H,h}). \tag{18}$$

10: **end for**

reasoning as in the previous section we may replace (17) by the following two problems: Find $(\delta \boldsymbol{e}_h, \delta e_h) \in (\delta \mathscr{V}_h, \delta \mathscr{W}_h)$ such that for all $(\delta \boldsymbol{v}_h, \delta q_h) \in (\delta \mathscr{V}_h, \delta \mathscr{W}_h)$

Algorithm 2 Alternating Schwarz extension to the numerical subgrid approach for Darcy's problem – second formulation.

1: Compute $\widetilde{\delta \boldsymbol{u}_h}$ for all coarse velocity basis functions, i.e., solve (13a) with $\boldsymbol{u}_H$ replaced by basis functions.
2: Set $(\boldsymbol{u}_h^0, p_h^0) \equiv (\boldsymbol{0}, 0)$.
3: **for** $j = 0, \ldots$ until convergence **do**
4: Steps 3:–7: of Algorithm 1
5: Solve (19a) for $(\delta \boldsymbol{e}_h, \delta e_h)$.
6: Set $(\boldsymbol{u}_h^{j+2/3}, p_h^{j+2/3}) = (\boldsymbol{u}_h^{j+1/3}, p_h^{j+1/3}) + (\delta \boldsymbol{e}_h, \delta e_h)$.
7: Solve (22) for $(\boldsymbol{e}_H, e_H)$.
8: Set $(\boldsymbol{u}_h^{j+1}, p_h^{j+1}) = (\boldsymbol{u}_h^{j+2/3} + \boldsymbol{e}_H + \widetilde{\delta \boldsymbol{u}}_h(\boldsymbol{e}_H), p_h^{j+2/3} + e_H + \widetilde{\delta p}_h(e_H))$.
9: **end for**

$$\begin{aligned} a_h(\delta \boldsymbol{e}_h, \delta \boldsymbol{v}_h) + b(\delta \boldsymbol{v}_h, \delta e_h) &= F(\delta \boldsymbol{v}_h) - a_h(\boldsymbol{u}_h^{j+\frac{1}{3}}, \delta \boldsymbol{v}_h) - b(\delta \boldsymbol{v}_h, p_h^{j+\frac{1}{3}}), \\ b(\delta \boldsymbol{e}_h, \delta q_h) &= -b(\boldsymbol{u}_h^{j+\frac{1}{3}}, \delta q_h). \end{aligned} \tag{19a}$$

Find $(\boldsymbol{e}_H, e_H) \in (\mathscr{V}_H, \mathscr{W}_H)$ such that for all $(\boldsymbol{v}, q) \in (\mathscr{V}_H, \mathscr{W}_H)$ we have

$$\begin{aligned} \widetilde{a}_H(\boldsymbol{e}_H, \boldsymbol{v}) + b(\boldsymbol{v}, e_H) &= F(\boldsymbol{v}) - a_h(\boldsymbol{u}_h^{j+\frac{1}{3}}, \boldsymbol{v}) - b(\boldsymbol{v}, p_h^{j+\frac{1}{3}}) - a_h(\delta \boldsymbol{e}_h, \boldsymbol{v}), \\ b(\boldsymbol{e}_H, q) &= -b(\boldsymbol{u}_h^{j+\frac{1}{3}}, q). \end{aligned} \tag{19b}$$

Here, (19a) and (19b) correspond to (13b) and (15), respectively, and analogous to (16), $(\boldsymbol{e}_{H,h}, e_{H,h})$ from (17) is obtained by

$$(\boldsymbol{e}_{H,h}, e_{H,h}) = (\boldsymbol{e}_H, e_H) + \left(\widetilde{\delta \boldsymbol{u}}_h(\boldsymbol{e}_H), \widetilde{\delta p}_h(\boldsymbol{e}_H)\right) + (\delta \boldsymbol{e}_h, \delta e_h). \tag{20}$$

Now, define

$$(\boldsymbol{u}_h^{j+\frac{2}{3}}, p_h^{j+\frac{2}{3}}) := (\boldsymbol{u}_h^{j+\frac{1}{3}}, p_h^{j+\frac{1}{3}}) + (\delta \boldsymbol{e}_h, \delta e_h).$$

Combining this with (18) and (20) we obtain

$$(\boldsymbol{u}_h^{j+1}, p_h^{j+1}) = (\boldsymbol{u}_h^{j+\frac{2}{3}}, p_h^{j+\frac{2}{3}}) + (\boldsymbol{e}_H, e_H) + (\widetilde{\delta \boldsymbol{u}}_h(\boldsymbol{e}_H), \widetilde{\delta p}_h(\boldsymbol{e}_H)). \tag{21}$$

We observe that due to (3a) and (3b) we may simplify (19b) to obtain the equality for all $(\boldsymbol{v}, q) \in (\mathscr{V}_H, \mathscr{W}_H)$

$$\begin{aligned} &\widetilde{a}_H(\boldsymbol{e}_H, \boldsymbol{v}) + b(\boldsymbol{v}, e_H) + b(\boldsymbol{e}_H, q) \\ &\qquad = F(\boldsymbol{v}) - a_h\left(\boldsymbol{u}_h^{j+\frac{2}{3}}, \boldsymbol{v}\right) - b(\boldsymbol{u}_h^{j+\frac{2}{3}}, q) - b(\boldsymbol{v}, p_h^{j+\frac{2}{3}}). \end{aligned} \tag{22}$$

Thus, we may rewrite Algorithm 1 in form of Algorithm 2.

Remark 2. Algorithm 2 also has a different interpretation than just being some equivalent formulation of Algorithm 1. It is straightforward to see that for $j = 0$, $(\boldsymbol{u}_h^{\frac{2}{3}}, p_h^{\frac{2}{3}}) = (\overline{\delta \boldsymbol{u}}_h, \overline{\delta p}_h)$, i.e. it is the solution of (13b). For $j \geq 1$ $(\boldsymbol{u}_h^{j+\frac{2}{3}}, p_h^{j+\frac{2}{3}})$ is the solution of (13b) with the homogeneous boundary conditions being replaced by (in general) inhomogeneous ones defined by $(\boldsymbol{u}_h^{j+\frac{1}{3}}, p_h^{j+\frac{1}{3}})$. Besides, (22) is of exactly the same form as (15). Thus, Algorithm 2 can be viewed as a subgrid algorithm that iteratively improves the local boundary conditions of the response to the right hand side.

Remark 3. As a byproduct of our consideration we have a subgrid approximation of the Darcy's equation. In this case the above algorithms reduce to an overlapping Schwarz domain decomposition method. Such methods were studied in details in [8, 10] where a convergence rate independent of H has been established.

5 Numerical Results

We consider the following example to test the numerical subgrid approach for Brinkman's problem and the enhanced version with alternating Schwarz iterations. The model problems has non-homogeneous boundary conditions, namely, $\boldsymbol{u} = \boldsymbol{g}$ on $\partial\Omega$. Extending this subgrid method to problems with non-homogeneous boundary data is possible under the condition that $\boldsymbol{g}$ is contained in the trace space of $\mathcal{V}_H$ on the boundary $\partial\Omega$.This has been elaborated in the PhD thesis of J. Willems, [13].

Example 1. We choose $\Omega = (0, 1)^2$ and

$$\boldsymbol{f} \equiv \boldsymbol{0}, \quad \boldsymbol{g} \equiv \begin{bmatrix} 1 \\ 0 \end{bmatrix}, \quad \mu = 1, \quad \kappa^{-1} = \begin{cases} 1e3 & \text{in dark regions,} \\ 1 & \text{in light regions,} \end{cases}$$

where the position of the obstacles is shown in Figure 4(a) (periodic case) and Figure 4(b) (media with small obstacles), and Figure 4(c) (media with relatively large vuggs), respectively.

We have chosen a fine mesh of 128×128 cells that resolve the geometry. For the subgrid algorithm we choose a coarse 8×8 mesh and each coarse-cell is further refined to 16×16 fine cells. On all figures we plot the numerical results for the velocity u_1 for Example 1.

On Figure 5 we report the numerical results for periodically arranged obstacles: Figure 5(a) shows the reference solution, computed on the global fine 128×128 grid, Figure 5(b) – the solution of the subgrid method, and Figure 5(c) – the solution after five iterations of overlapping Schwarz domain decomposition method (Schwarz DD). The relative L^2-norm of the error for the the subgrid solution shown in Figure 5(b) is $7.14e-2$, while after five Schwarz iterations (see Figure 5(c)) the L^2-norm of the error is an order of magnitude better.

Likewise, on Figure 6 we show the numerical results for the two geometries shown on Figures 4(b) and 4(c). The first row represents the reference solution

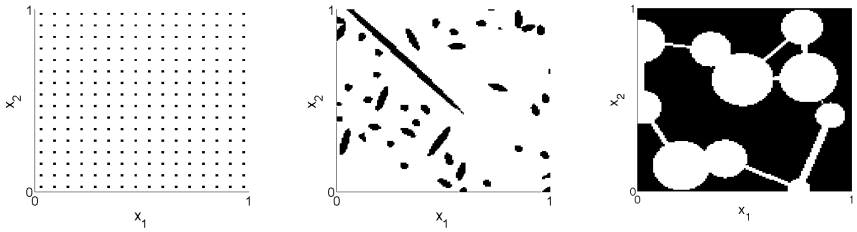

(a) Periodic geometry. (b) Media with obstacles. (c) Media with large vuggs.

Fig. 4. Three test geometries. The dark regions indicate obstacles or porous media, i.e. κ^{-1} is large, and the light regions indicate (almost) free flow regions, i.e. κ^{-1} is small.

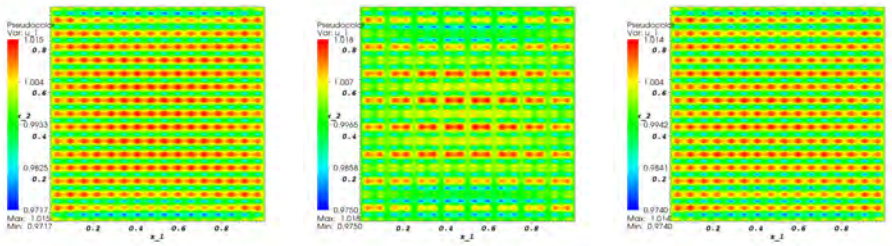

(a) Reference solution. (b) Subgrid solution. (c) Schwarz DD, 5 it.

Fig. 5. Velocity u_1 for media with periodically arranged obstacles of Figure 4(a)

computed on the global fine grid with 128×128 cells. In the second row we give the solution of the subgrid method and in the third row we show the solution obtained after few Schwarz overlapping domain decomposition iterations. In all cases we clearly see the error of the subgrid solution along the coarse-grid boundaries. This error is due to the prescribed zero values for the fine-grid velocity on the coarse-grid boundaries and is characteristic for the multiscale methods (e.g. [14]). As we see in the numerical experiments, few Schwarz iterations substantially decrease the error. For the geometry shown on Figure 4(c) the improvement is achieved after just one iteration, while for the geometry shown on Figure 4(b) the substantial improvement is achieved after 10 iterations. In all cases the approximate solution of Schwarz overlapping method obtained in few iterations is very close to the reference one.

Acknowledgments. The research of O. Iliev was supported by DAAD-PPP D/07/10578 and award KUS-C1-016-04, made by King Abdullah University of Science and Technology (KAUST). R. Lazarov has been supported by award KUS-C1-016-04, made by KAUST, by NSF Grant DMS-0713829, and by the European School for Industrial Mathematics (ESIM) sponsored by the Erasmus Mundus program of the EU. J. Willems was supported by DAAD-PPP D/07/10578, NSF Grant DMS-0713829, and the Studienstiftung des deutschen Volkes (German National Academic Foundation). Part of the research was per-

formed during the visit of O. Iliev to Texas A&M University. The hospitality of the Institute of Applied Mathematics and Computational Science, funded by KAUST, and the Institute for Scientific Computing are gratefully acknowledged.

The authors express sincere thanks to Dr. Yalchin Efendiev for his valuable comments and numerous discussion on the subject of this paper.

References

1. Allaire, G.: Homogenization of the Navier-Stokes Equations in Open Sets Perforated with Tiny Holes. I: Abstract Framework, a Volume Distribution of Holes. Arch. Rat. Mech. Anal. 113 (3), 209-259 (1991)
2. Allaire, G.: Homogenization of the Navier-Stokes Equations in Open Sets Perforated with Tiny Holes. II: Non-critical Size of the Holes for a Volume Distribution and a Surface Distribution of Holes, Arch. Rat. Mech. Anal., 113, (3), 261-298 (1991)
3. Angot, Ph.: Analysis of Singular Perturbations on the Brinkman Problem for Fictitious Domain Models of Viscous Flows, Math. Methods Appl. Sci. 22 (16), 1395-1412 (1999)
4. Arbogast, T.: Analysis of a Two-Scale, Locally Conservative Subgrid Upscaling for Elliptic Problems. SIAM J. Numer. Anal. 42 (2), 576-598 (2004)
5. Brezzi, F. and Fortin, M.: Mixed and Hybrid Finite Element Methods, Volume 15 of Springer Series in Comput. Mathematics, Springer-Verlag, New York (1991)
6. Brinkman, H.C.: A Calculation of the Viscose Force Exerted by a Flowing Fluid on a Dense Swarm of Particles. Appl. Sci. Res. A1, 27-34 (1947)
7. deal.II: A Finite Element Differential Equations Analysis Library, `http://www.dealii.org/`
8. Ewing, R. and Wang, J.: Analysis of the Schwarz Algorithm for Mixed Finite Element Methods, Math. Modelling and Numer. Anal., 26 (6), 739-756 (1992)
9. Hornung, U., editor: Homogenization and Porous Media, Volume 6 of Interdisciplinary Applied Mathematics. Springer, 1st edition, (1997)
10. Mathew, T.: Schwarz Alternating and Iterative Refinement Methods for Mixed Formulations of Elliptic Problems, Part II: Convergence Theory, Numer. Math. 65, 469-492 (1993)
11. Ochoa-Tapia, J.A. and Whitaker, S.: Momentum Transfer at the Boundary Between a Porous Medium and a Homogeneous Fluid. I. Theoretical development. Int. J. Heat Mass Transfer, 38, 2635-2646 (1995)
12. Wang, J. and Ye, X.: New Finite Element Methods in Computational Fluid Dynamics by $H(div)$ Elements. SIAM J. Numer. Anal. 45 (3), 1269-1286 (2007)
13. Willems, J.: *Numerical Upscaling for Multi-Scale Flow Problems*, Ph.D. Thesis, Technical University of Kaiserslautern, (2009)
14. Wu, X.H., Efendiev, Y., and Hou, T.Y.: Analysis of Upscaling Absolute Permeability, Discrete Contin. Dyn. Syst., Ser B, 2, 185-204 (2002)

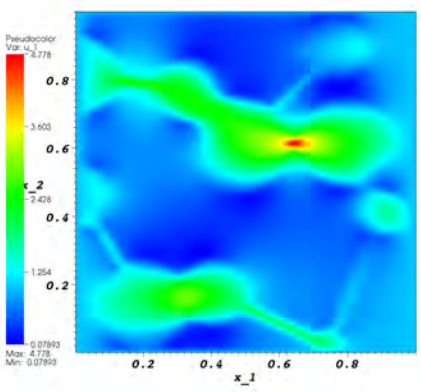

(a) Reference solution.

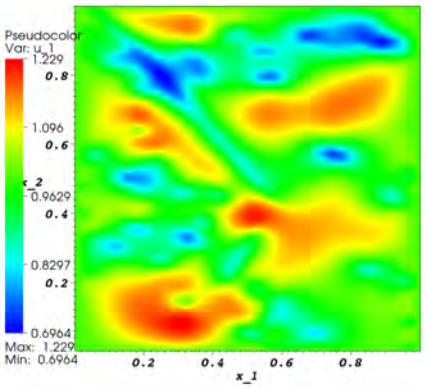

(b) Reference solution.

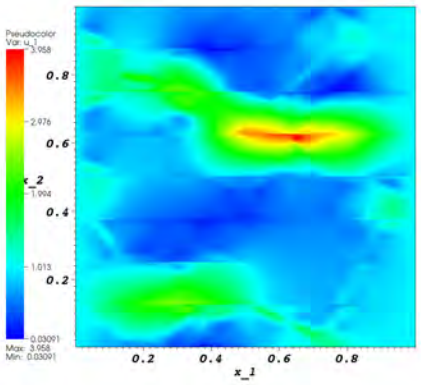

(c) Subgrid FE solution.

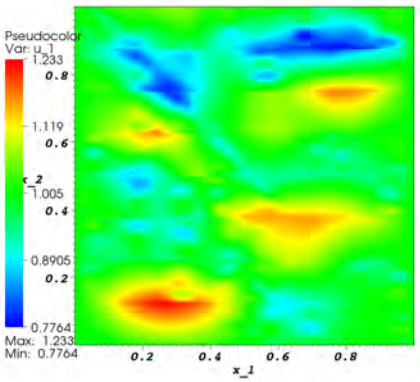

(d) Subgrid FE solution.

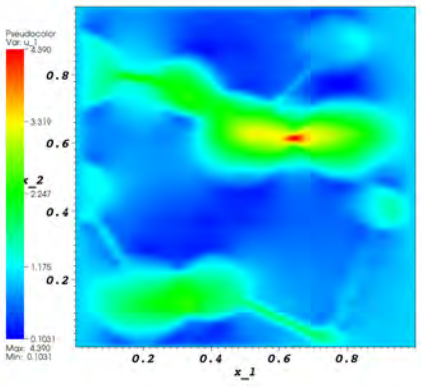

(e) Schwarz DD after 1 iteration

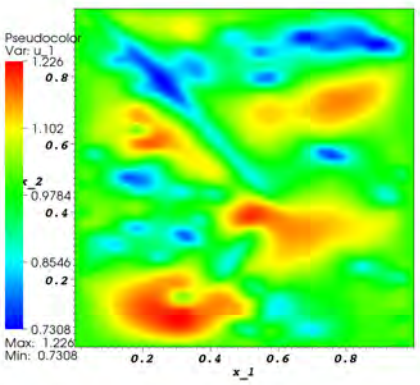

(f) Schwarz DD after 10 iterations

Fig. 6. Velocity component u_1 for Example 1; on the left – the results for geometry of Figure 4(b) and the right row – the results for geometry of Figure 4(c)